Proatherogenic Effects of the Cholesterol Ozonolysis Products, Atheronal-A and Atheronal-B †

ARTICLE *in* BIOCHEMISTRY · JUNE 2006

Impact Factor: 3.02 · DOI: 10.1021/bi0604330 · Source: PubMed

8 AUTHORS, INCLUDING:

Roger Galve
Spanish National Research Council
32 PUBLICATIONS **926** CITATIONS
SEE PROFILE

Jorge Nieva
Keck School of Medicine USC
48 PUBLICATIONS **2,120** CITATIONS
SEE PROFILE

Daniel Witter
University of Florida
7 PUBLICATIONS **95** CITATIONS
SEE PROFILE

Paul Wentworth
The Scripps Research Institute
70 PUBLICATIONS **2,229** CITATIONS
SEE PROFILE

Proatherogenic Effects of the Cholesterol Ozonolysis Products, Atheronal-A and Atheronal-B[†]

Cindy Takeuchi,[‡] Roger Galvé,[‡] Jorgé Nieva,[§] Daniel P. Witter,[||] Anita D. Wentworth,[‡] Ryan P. Troseth,[‡] Richard A. Lerner,[‡] and Paul Wentworth, Jr.*[,‡,||]

Departments of Chemistry and Molecular and Experimental Medicine, The Scripps Research Institute, 10550 North Torrey Pines Road, La Jolla, California 92037, The Scripps−Oxford Laboratory, Oxford Glycobiology Institute, Department of Biochemistry, University of Oxford, South Parks Road, Oxford OX1 3QU, United Kingdom

Received March 3, 2006

ABSTRACT: The proatherogenic properties of the cholesterol 5,6-*seco*sterols (atheronal-A and atheronal-B), recently discovered in atherosclerotic arteries, have been investigated in terms of their effects on monocyte/macrophage function. A fluorescent analogue of atheronal-B (**1**) (50 μM), when cultured in either aqueous buffer (PBS) or in media containing fetal calf serum (10%), is rapidly taken-up into cultured macrophage (J774.1 or RAW 264.7) cells and accumulates at perinuclear sites (within 1 h). Co-incubation of macrophage cells (J774.1) with atheronal-A (25 μM) and atheronal-B (25 μM) when complexed with low-density lipoprotein (LDL) (100 μg/mL) leads to a significant upregulation of scavenger receptor class A (∼3-fold increase relative to LDL alone, $p < 0.05$) but not CD36, showing that cultured macrophages respond to LDL-complexed atheronals in a manner highly analogous to acetylated LDL rather than oxidized LDL. Both atheronal-A and atheronal-B in solution exhibit a dose-dependent (0−25 μM) induction of chemotaxis of cultured macrophages ($p < 0.001$). When complexed with LDL (100 μg/mL), atheronal-A (but not atheronal-B) induces a dose-dependent (0−25 μM, $p < 0.05$) upregulation of the cell-surface adhesion molecule endothelial (E)-selectin on vascular endothelial cells (HUVECs). LDL (100 μg/mL) complexed atheronal-B (25 μM) but not atheronal-A induces cultured human monocytes (THP-1) to differentiate into macrophage cell lineage. When these in vitro data are taken together with the already known effects of cholesterol 5,6-*seco*sterols on foam cell formation and macrophage cytotoxicity, the atheronals possess biological effects that if translated to an in vivo setting could lead to the recruitment, entrapment, dysfunction, and ultimate destruction of macrophages, with the major leukocyte player in inflammatory artery disease. As such, the atheronal molecules may be a new association, in the already complex inter-relationship, between inflammation, cholesterol oxidation, the tissue macrophage, and atherosclerosis.

Atherosclerosis, formerly considered to be a disease of lipid storage, is now accepted as having a pervasive inflammatory component from initiation through progression to ultimate thrombotic complications (*1*). Clinical studies have shown that this emerging biology of inflammation in atherosclerosis applies directly to human patients. There is also increasing evidence revealing that elevation of markers of inflammation predicts outcomes of patients with acute coronary syndromes, independently of myocardial damage (*2*, *3*).

We have recently discovered that hitherto unknown biological cholesterol oxidation products, cholesterol 5,6-*seco*sterols, termed atheronal-A and atheronal-B, are present within atherosclerotic plaque material at the time of endarterectomy (Figure 1) (*4*). Atheronal-B is also present in human plasma and was found to be significantly elevated in a small cohort of human patients whose atherosclerosis disease state was sufficient to warrant carotid endarterectomy, relative to a cohort of patients with no known cardiovascular disease. Further studies have shown that both atheronal-A and atheronal-B trigger foam cell formation, cause apo-B_{100} misfolding, and are cytotoxic to cultured macrophages (*4*).

From a strictly chemical point of view, the atheronals are unique among biologically relevant cholesterol oxidation products (oxysterols) because they result from an oxidative cleavage of the steroid framework, whereas all other oxysterols are products of peripheral oxidation of an otherwise intact steroid nucleus (*5*). The understanding of how specific chemistry, biochemistry, and environment may all contribute to the in vivo levels of these molecules is an area of intensive research in our laboratory. However, it is well-known that chemical oxidation routes to atheronal-A generally proceed via the reaction between cholesterol and ozone. In 1993, Pryor and co-workers (*6*) showed that atheronal-A, system-

[†] This work was supported by the ALSAM Foundation and the Skaggs Institute for Research and Novartis Pharma AG (SFP-1551). R.G. was supported by a fellowship from La Secretaria de Estado de Educación y Universidades and El Fondo Social Europeo. D.W. was supported by a Scripps Florida−Oxford predoctoral scholarship.

* To whom correspondence should be addressed. Telephone: +1-858-784-2576. Fax: +1-858-784-2593. E-mail: paulw@scripps.edu or paul.wentworth@bioch.ox.ac.uk.

[‡] Department of Chemistry, The Scripps Research Institute.

[§] Department of Molecular and Experimental Medicine, The Scripps Research Institute.

[||] University of Oxford.

10.1021/bi0604330 CCC: $33.50
Published on Web 05/17/2006

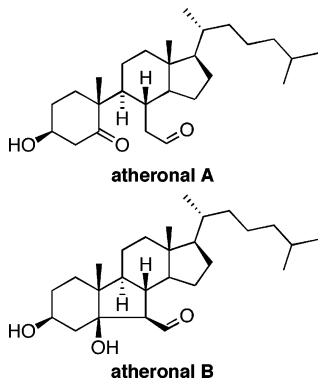

FIGURE 1: Cholesterol 5,6-*seco*sterols, atheronal-A and atheronal-B.

atically named 3β-hydroxy-5-*oxo*-5,6-*seco*cholestan-6-al, is a major product of cholesterol ozonolysis. Atheronal-A is converted into atheronal-B, systematically named 3β-hydroxy-5β-hydroxy-B-norcholestane-6β-carboxaldehyde, by an intramolecular aldolization process (*6*), and as we have shown, this reaction occurs very rapidly in the presence of blood fractions and atheroma (*4*). In fact, atheronal-A is converted into atheronal-B so rapidly in whole blood that immediately upon the addition of atheronal-A to blood only atheronal-B is detectable (*4*). Thus, because atheronal-A is directly derived from ozonolysis of cholesterol and aldolization of atheronal-A occurs so smoothly in biological systems, both atheronal-A and atheronal-B in vivo are termed cholesterol ozonolysis products.

The biological origin of these cholesterol oxidation products remains unclear; however, we have observed that the levels of atheronal-A are significantly increased ($p < 0.05$) within excised plaque material upon the activation of the oxidative burst of the residual phagocytes present in plaque. Thus, these molecules seem to be derived in part from the juxtaposition of high cholesterol levels with activated inflammatory cells, a convergence that is almost unique to the atheromatous plaque (*4*). Recent studies by us and others have shown that the atheronals cause misfolding and aggregation of β-amyloid protein (*8*) and cause membrane destabilization by binding to phosphatidylethanolamine (*9*).

Given the fact that we discovered the atheronals in atherosclerotic arteries and that other oxysterols are known to possess proatherosclerotic profiles (*10*−*13*), we have investigated whether these cholesterol 5,6-*seco*sterols possess biological effects in vitro that may contribute to atherogenesis in vivo. Herein, we report that, on the basis of data from in vitro experiments, the atheronals possess significant atherogenic potential. Atheronals accelerate/stimulate a number of models of processes considered critical to early atherosclerotic lesion formation, including macrophage recruitment, endothelial cell adhesion molecule upregulation, monocyte differentiation into macrophages, and macrophage foam cell formation via scavenger receptor A (SR-A)[1] upregulation.

MATERIALS AND METHODS

Synthetic Methods. Unless otherwise stated, all reactions were performed under an inert atmosphere with dry reagents, solvents, and flame-dried glassware. All starting materials were purchased from Aldrich, Sigma, Fisher, or Lancaster and used as received. All flash column chromatography was performed using silica gel 60 (230−400 mesh). Preparative thin-layer chromatography (TLC) was performed using Merck (0.25, 0.5, or 1 mm) coated silica gel Kieselgel 60 F254 plates. Atheronal-A (3β-hydroxy-5-*oxo*-5,6-*seco*-cholestan-6-al) and atheronal-B (3β-hydroxy-5β-hydroxy-B-norcholestane-6β-carboxaldehyde) were synthesized as previously described (*4*).

*Synthesis of 3β-Hydroxy-5-cholenic Acid, Dansyl Hydrazide (**2**)*. To a stirred solution of 5-cholenic acid-3β-ol (50 mg, 0.13 mmol) and 5-(dimethylamino)-1-naphthalenesulfonamide **3** (dansylamide, 68 mg, 0.27 mmol) in dioxane (5 mL) was added 1-[3-(dimethylamino)propyl]-3-ethylcarbodiimide hydrochloride (EDCI, 39 mg, 0.20 mmol) and 4-(dimethylamino)pyridine (DMAP, 5 mg, 0.04 mmol). The reaction mixture was stirred under an inert atmosphere for 24 h before quenching by the addition of methanol (5 mL). The resulting precipitate was collected by filtration to yield the title compound as a yellow solid (32.5 mg, 40%). ^{1}H NMR ($CDCl_3$, 400 MHz) δ: 8.49 (d, $J = 8.8$ Hz, 1H), 8.37 (d, $J = 7.2$ Hz, 1H), 8.15 (d, $J = 8.4$ Hz, 1H), 7.50 (dd, $J = 8.4$, 7.6 Hz, 1H), 7.48 (dd, $J = 8.4$, 7.6 Hz, 1H), 7.10 (d, $J = 7.6$ Hz, 1H), 5.25 (m, 1H), 2.80 (s, 6H), 0.90 (s, 3H), 0.69 (d, $J = 6.4$ Hz, 3H), 0.43 (s, 3H). ^{1}H NMR [dimethyl sulfoxide (DMSO)-d_6, 400 MHz] δ: 8.50 (d, $J = 8.5$ Hz, 1H), 8.27 (d, $J = 7.3$ Hz, 1H), 8.21 (d, $J = 8.8$ Hz, 1H), 7.65 (pt, $J = 8.0$ Hz, 1H), 7.60 (pt, $J = 8.1$ Hz, 1H), 7.24 (d, $J = 7.6$ Hz, 1H), 5.23 (bd, 1H), 4.60 (bd, 1H), 3.34 (bs, 1H), 2.81 (s, 6H), 0.90 (s, 3H), 0.65 (d, $J = 5.6$ Hz, 3H), 0.32 (s, 3H). ^{13}C NMR (DMSO-d_6, 100 MHz) δ: 171.6, 151.5, 141.1, 134.2, 131.0, 130.6, 128.8 (2C)*, 128.2, 123.3, 120.3, 118.0, 115.0, 69.9, 55.9, 55.1, 49.4, 45.0 (2C)*, 42.2, 41.6, 39.0**, 36.8, 36.4, 34.2, 32.4, 31.3, 31.2, 30.2, 27.3 (2C)*, 23.7, 20.5, 19.0, 17.8, 11.3. HRMALDIFTMS calcd for $C_{36}H_{51}N_2O_4S$ (M + H), 607.3564; found, 607.3535. $R_f = 0.33$ [diethyl ether (neat)]. (*) The 2C denotes that this signal is believed to correspond to two carbon signals by comparison to starting materials (analyzed by 2D experiments). (**) This carbon signal was revealed by a DEPT 135 experiment.

*Synthesis of Aldol, Dansylhydrazide (**1**)*. Dansyl hydrazide **1** was prepared in two steps via an intermediate keto aldehyde cholenic acid. In step 1, a solution of 5-cholenic acid-3β-ol (300 mg, 0.80 mmol) in methylene chloride/methanol (50 mL, 9:1) cooled to 0 °C was treated with a stream of ozone for ca. 5 min until no starting material could be detected by TLC [ethyl acetate/hexane (4:1)]. The nitrogen-purged reaction mixture was evaporated to dryness before the addition of acetic acid (AcOH, 30 mL), H_2O (1.5 mL), and zinc dust (300 mg, 4.6 mmol). The resulting suspension was stirred at ambient temperature for 2 h before partitioning by the addition of H_2O and methylene chloride. After the organic

[1] Abbreviations: LDL, low-density lipoprotein; ox-LDL, oxidized low-density lipoprotein; CuOx-LDL, Cu^{II}-oxidized low-density lipoprotein; PBS, phosphate-buffered saline; DMSO, dimethyl sulfoxide; DMEM, Dulbecco's modified Eagle's media; FCS, fetal calf serum; BSA, bovine serum albumin; LTB-4, leukotriene B4; MCP-1, monocyte chemoattractant protein 1; VCAM-1, vascular cell adhesion molecule 1; ICAM-1; intercellular adhesion molecule 1; LDH, lactate dehydrogenase; EDTA, ethylenediaminetetraacetic acid; SR-A, macrophage scavenger receptor class A; TBARS, thiobarbituric-acid-reactive substances; M-CSF, monocyte colony-stimulating factor; GM-CSF, granulocyte-macrophage colony-stimulating factor; 7-KC, 7-ketocholesterol.

fraction was dried ($MgSO_4$) and concentrated in vacuo, the residue was purified using silica gel chromatography [ethyl acetate/hexane/AcOH (40:27:1)] to furnish the intermediate keto aldehyde cholenic acid as a white solid (140 mg, 43%). ^{1}H NMR ($CDCl_3$, 400 MHz) δ: 9.60 (s, 1H), 4.47 (s, 1H), 3.40 (dd, J = 13.6, 4.0 Hz, 1H), 1.00 (s, 3H), 0.91 (d, J = 6.4 Hz, 3H), 0.67 (s, 3H). ^{13}C NMR ($CDCl_3$, 100 MHz) δ: 218.7, 202.9, 179.8, 70.9, 55.5, 54.1, 52.5, 46.4, 44.0, 42.4, 42.1, 39.6, 35.1, 34.5, 34.0, 30.8, 30.4, 27.5, 27.3, 25.1, 22.8, 17.9, 17.4, 11.4. HRMALDIFTMS calcd for $C_{24}H_{38}O_5Na$ (M + Na), 429.2611; found, 429.2611. R_f = 0.20 [ethyl acetate/hexane (1:1)].

Under an inert atmosphere, a stirring solution of the intermediate keto aldehyde cholenic acid (27 mg, 66 μmol) in reaction-grade dioxane (6 mL) was treated sequentially with dansyl amide (49.5 mg, 0.20 mmol), EDCI (25.2 mg, 0.13 mmol) and DMAP (10 mg, 82 μmol). After 9 h, the reaction mixture was concentrated in vacuo and purified by preparative TLC at 0.25 mm [diethyl ether/hexane (8:2)] to afford dansyl hydrazide **1** as a yellow solid (8 mg, 19%). ^{1}H NMR ($CDCl_3$, 600 MHz) δ: 9.69 (d, J = 2.8 Hz, 1H), 8.61 (d, J = 8.2 Hz, 1H), 8.49 (d, J = 7.3 Hz, 1H), 8.20 (d, J = 8.3 Hz, 1H), 7.58 (pq, J = 8.3 Hz, 2H), 7.18 (d, J = 7.3 Hz, 1H), 4.13 (bm, 1H), 3.52 (s, 1H), 2.89 (s, 6H), 0.90 (s, 3H), 0.75 (d, J = 7.3 Hz, 3H), 0.57 (s, 3H). ^{13}C NMR ($CDCl_3$, 150 MHz) δ: 204.6, 171.1, 152.3, 132.3, 131.9, 129.8, 129.5 (2C)*, 128.8, 123.2, 117.9, 115.2, 84.2, 67.4, 63.8, 56.0, 55.3, 50.3, 45.5, 45.4, 45.4, 44.7, 44.2, 39.8, 39.6, 34.9, 30.3, 28.1, 27.9 (2C)*, 26.7, 24.4, 21.5, 18.4, 18.2, 12.4. HRMALDIFTMS calcd for $C_{36}H_{51}N_2O_6S$ (M + H), 639.3462; found, 639.3470. R_f = 0.13 [diethyl ether (neat)]. (*) The 2C denotes that this signal corresponds to two carbon signals by comparison to starting materials (analyzed by 2D experiments).

Cu-Mediated Oxidation of Low-Density Lipoprotein (LDL). Cu^{II}-Oxidized low-density lipoprotein (CuOx-LDL) was generated by dialyzing human LDL (100 μg/mL) (CalBiochem, La Jolla, CA) in $CuSO_4$ (5 μM) against phosphate-buffered saline (PBS) at pH 7.4 and 37 °C for 12 h as previously described (*14*). LDL oxidation was assessed by the extent of thiobarbituric-acid-reactive substances (TBARS) (*15*). In brief, the oxidized LDL sample or control LDL sample was treated with 2 parts trichloroacetic acid (3.8%, w/v) and 2-thiobarbituric acid (0.1%, w/v) in HCl (0.06 N) and 0.2 parts of an aqueous SDS solution (0.625 mM) and then heated to 95 °C for 30 min. After cooling, the sample was extracted twice with *n*-butanol (100 μL), and the absorbance of the extract was measured at 532 nm. Quantification was by interpolation from a standard curve generated by malondialdehyde bis(dimethyl acetal) (Aldrich).

Complexation of Atheronal-A or Atheronal-B with LDL. In a typical experiment, a solution of atheronal-A (25 μM, final concentration) or atheronal-B (25 μM, final concentration) in DMSO [0.4% (v/v), final concentration] is added to human LDL (100 μg/mL; CalBiochem, La Jolla, CA) in PBS. The resultant mixture is incubated at room temperature for 2 h under an inert atmosphere and then dialyzed against PBS. Note: Under such conditions, >90% of the atheronals remains associated with LDL as quantified by our previously developed RP-HPLC (*4*) analysis of the dialysate.

Cell Culture. Human abdominal aorta endothelial (HAAE-1) cell line (CRL-2472), J774A.1 murine tissue macrophage cell line (TIB-67), and monocytic cell lines U-937 histiocytic lymphoma (CRL-1593.2) and THP-1 acute monocytic leukemia (TIB-202) were obtained from ATCC (*16*−*19*). All cell lines were cultured in ATCC-recommended media with 10% fetal calf serum (FCS). Cells were incubated in a controlled atmosphere at 37 °C, with 5 or 7% CO_2. The release of lactate dehydrogenase (LDH) from cells was used to measure cytotoxicity as previously described (*5*).

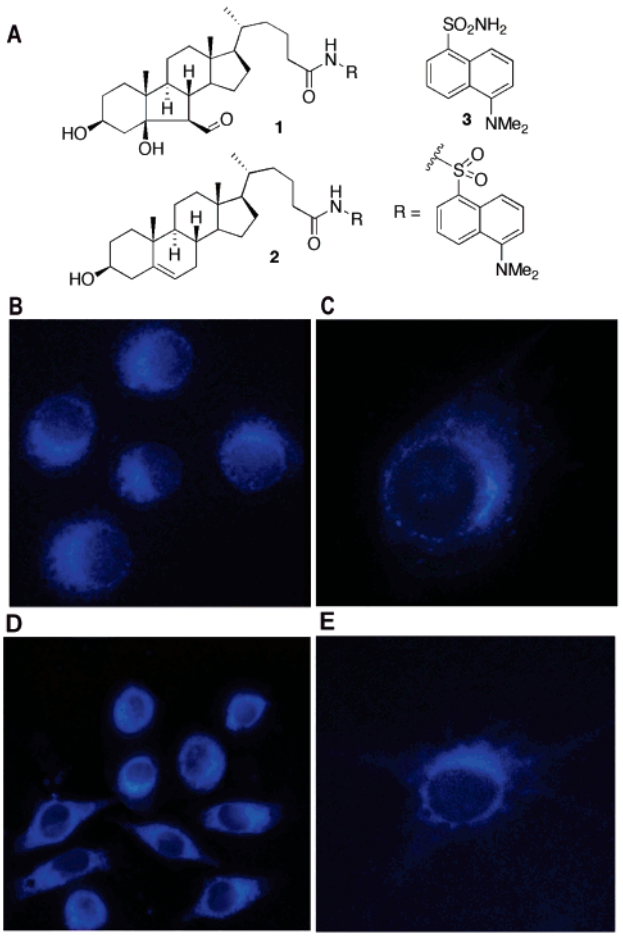

FIGURE 2: Macrophage uptake and localization of dansyl atheronal-B analogue **1**. (A) Cell-uptake experiments were performed with the synthetic fluorescent dansyl atheronal-B analogue **1**. The dansyl cholesterol analogue **2** was studied as a control. (B) Fluorescence microscopy of cultured macrophage cells (J774A.1) treated with **1** (50 μM) in PBS for 5 min (100×). (C) Fluorescence microscopy of cultured macrophage cells (J774A.1) treated with **1** (50 μM) for 1 h (200×). (D) Cultured macrophages treated with **1** (50 μM) in media with FCS (10%) for 5 min (60×). (E) Cultured macrophages (RAW 264.7) treated with **1** (50 μM) in media with FCS (10%) for 60 min (100×). Note: No uptake of **2** or dansyl amide **3** was observed during this experiment with either cell line (data not shown). After treatment, cells were fixed in 95% cold methanol and mounted in glycerol. These data were collected using a filter set combination (excitation) DAPI 360/40 and (emission) 457/50.

Atheronal Uptake into Cultured Macrophages. For the images shown in parts B and C of Figure 2, murine macrophage J774A.1 cells were plated in 8-well chambered slides. Cells were gently washed twice with PBS at pH 7.4; then either dansylated atheronal-B analogue **1** (50 μM), dansylated cholesterol analogue **2** (50 μM), or dansyl hydrazine (50 μM), in media without FCS and with DMSO as a cosolvent (0.05%, v/v) was added; and the cells were then incubated at 37 °C for either 5 or 60 min. Media was

then removed by aspiration, and cells were fixed immediately in 95% ice-cold methanol for 5 min. Cells were mounted in glycerol containing Antifade reagent (Molecular Probes). Fluorescence images were documented using a DeltaVision deconvolution microscope (API, Issaquah, WA) equipped with a Photometrics CH350L liquid-cooled CCD camera attached to an Olympus IX_70 inverted microscope. These data were collected using a 60× oil immersion objective lens (NA 1.4) and a filter set combination (excitation) DAPI 360/40 nm and (emission) 457/50 nm. All images were deconvoluted using constrained iterative algorithms (10 iterations) of DeltaVision software (softWoRx, version 2.5). The deconvoluted images were subsequently processed using softWoRx, version 2.5. For the images shown in parts D and E of Figure 2, murine macrophage RAW 264.7 (ECACC 91062702) cells were grown in RPMI (Gibco) with 10% FCS at 37 °C with 5% CO_2. For fluorescence imaging, cells were incubated on cover slips in 6-well chambered plates (Costar) for 12 h, gently washed 3 times in PBS at pH 7.4, and incubated with a dansylated atheronal-B analogue **1** (50 μM) in RPMI with 10% FCS for 5, 15, 30, and 60 min. A solution of atheronal-B analogue **1** was then added in DMSO [final DMSO, 0.05% (v/v)]. Media was removed by aspiration, and cells were washed twice with PBS, followed by fixing in paraformaldehyde (3.7% in PBS) for 10 min. Cover slips were mounted in MOWIOL 4-88 (Calbiochem). Microscopy was performed using an inverted Zeiss Axioscope 2 Plus fluorescence microscope, and images were obtained with a Zeiss Axiocam digital camera using Axiovision software (version 3.1). The data were collected using a 63× oil immersion lens and DAPI filter (excitation 360/emission 460), and images were processed with Axiovision software and Adobe software (Photoshop 6.0).

Macrophage Scavenger Receptor Expression. Murine-cultured macrophage cells (J774A.1) were serum-starved overnight in media containing 0.5% bovine serum albumin (BSA). Cells (1×10^6) were then incubated with either vehicle, atheronal-A/LDL (25 μM, 100 μg/mL), atheronal-B/LDL (25 μM, 100 μg/mL), LDL (100 μg/mL), or CuOx-LDL (100 μg/mL) for specified times and washed twice with PBS. Note: Atheronal-complexed LDL was prepared as described above. Cells were harvested by scraping and fixed with 6% paraformaldehyde for 20 min. Then, cells were resuspended in PBS containing heat-inactivated FCS (2%, v/v), NaN_3 (0.05%, w/v), and an appropriate primary antibody, antibody conjugate, or isotype control (1:100 dilution) and incubated on ice for 30 min. Expression of either CD36 or SR-A was determined with CD36 (BD Biosciences Pharmingen, San Diego, CA) and CD204 (Serotec, Oxford, U.K.) specific monoclonal antibodies (*11*, *20*), respectively. After the primary antibody-treated cells were washed, secondary antibodies were added and cells were again washed and then analyzed on a FACS calibur 2 (Becton Dickinson, Sparks, MD) flow cytometer with analysis by CellQuant software. Results are expressed as mean fluorescence intensity ± standard error of the mean (SEM) of at least duplicate determinations. Significance was determined using a student two-tail *t* test, with (*) $p < 0.05$, (**) $p < 0.01$ versus the control.

Macrophage Chemotaxis and Migration. Chemotaxis and invasion assays were performed using a modified Boyden chamber migration assay (*21*, *22*) in MultiScreen-MIC plates (Millipore, Billerica, MA) with poly(vinylpyrrolidinone)-free polycarbonate membranes (5 μm pore size). Murine macrophage (J774A.1) cells were washed and resuspended in serum-free Dulbecco's modified Eagle's media (DMEM) containing BSA (0.2%) at 1×10^6 cells/mL. An aliquot of cells (50 μL) was then added to the upper well of the MIC plate, and an aliquot (150 μL) of either vehicle [serum-free DMEM containing BSA (0.2%) and DMSO (0.5%)] or cholesterol (25 μM), atheronal-A (25 μM), atheronal-B (25 μM), and C5a (10 nM) in the vehicle [serum-free DMEM containing BSA (0.2%) and DMSO (0.5%)] was added to the lower well of the microchamber. The plate was then incubated for 4 h at 37 °C in an 8% CO_2 atmosphere. After cells were wiped off the upper side of the membrane, cells adherent to the lower side were visualized by either staining and phase-contrast microscopy or fluorescence. Cells that had adhered to the membrane were stained using a DiffQuik staining kit (Dade Behring, Newark, DE). Each experiment was performed in triplicate, and the numbers of migrating cells were counted in five fields at 200×. Cells harvested with PBS−ethylenediaminetetraacetic acid (EDTA) for fluorescent labeling were washed 2 times with PBS and then resuspended in serum-free medium containing calcein AM (5 μM). Cells were incubated for 30 min at 37 °C in a 5% CO_2 atmosphere with gentle intermittent mixing. Calcein-AM-labeled cells were washed twice, and calcein fluorescence ($\lambda_{excitation} = 390$ nm, and $\lambda_{emission} = 460$ nm) was measured using a SPECTRAmax GEMINI dual-scanning microplate spectrofluorometer. Fluorescence measurements were quantified by comparison to a standard curve, generated by a dilution of calcein-AM-stained cells in PBS/BSA. For measuring the atheronal-B concentration-dependent (0−10 μg/mL) effect on cell-migration experiments, the method was the same as above with the exception that the macrophage cells were labeled with calcein AM prior to commencing the migration assay.

Endothelial Cell Adhesion Molecule Expression. Endothelial cell-surface adhesion molecule expression was studied on cultured HAAE-1 cells and was quantified by the enzyme-linked immunosorbent assay (ELISA), using anti-human CD54 [intercellular adhesion molecule 1 (ICAM-1)], CD106 [vascular cell adhesion molecule 1 (VCAM-1)], and CD62E [endothelial (E)-selectin] antibodies (Leinco Technologies, Inc., St. Louis, MO). The ELISA method was modified from previously described procedures (*23*−*25*). Thus, cells were cultured in 96-well plates and then incubated with either vehicle or LDL (1−3 nmol/mg of protein), CuOx-LDL (TBARS, 80−100 nmol/mg of protein), atheronal-A (25 μM)/LDL, and atheronal-B (25 μM)/LDL (100 μg/mL protein) in the vehicle for appropriate times and washed once with PBS. Cells were then incubated with antibodies to VCAM-1, E-selectin, or ICAM-1 diluted 1:400 in PBS containing 5% FCS at 37 °C for 30 min. Wells were washed 2 times with PBS and then incubated with horseradish peroxidase (HRP)-conjugated goat anti-mouse IgG (Southern Biotechnology Associates, Birmingham, AL) in PBS/5% FCS at 37 °C for 30 min. The wells were then washed 4 times with PBS; H_2O_2/3,3′,5,5′-tetramethylbenzidine peroxidase substrate (Pierce Chemical, Rockford, IL) was added; and the plate was allowed to stand for 30 min in the dark. The reaction was stopped by the addition of H_2SO_4 (25 μL, 8 N), and the absorbance at 450 nm was measured on a

microtiter plate reader. Each experiment was performed in triplicate, and the data are reported as the mean ± SEM as a percentage of the expression level of the vehicle. To study the effect of the atheronal-B concentration (5−50 μM) on E-selectin expression, the assay was performed in an identical fashion as described above, with each point being the mean ± SEM of at least duplicate measurements.

Monocyte Morphology Changes. Human monocytes (THP-1) cultured in suspension were plated in 8-well chambered slides. Cells were incubated with either vehicle (DMEM and 0.4% DMSO) or cholesterol, 7-ketocholesterol (7-KC), atheronal-A or atheronal-B (12 and 25 μM) in the vehicle and examined for morphological changes during a 7 day incubation at 37 °C. Media with appropriate treatment compounds was replaced after 4 days. After 4 days of treatment, morphologic changes of the adherent cells were assessed by phase-contrast microscopy and photographed using an Olympus Microfire digital camera.

Statistical Analyses. In all cases, data were statistically analyzed by a two-tailed, paired Student's *t* test in Microsoft EXCEL software. A value of $p \leq 0.05$ was taken as significant. Data are reported as the mean ± SEM unless otherwise stated.

RESULTS AND DISCUSSION

Treatment of live cultured macrophages (J774.1 or RAW 264.7) with a fluorescent cholenic acid analogue of atheronal-B **1** (25 μM) (Figure 2A), either in PBS (in the absence of lipoproteins) or in media containing 10% FCS, leads to a rapid time-dependent uptake of **1** into the cells, as measured by fluorescence microscopy (Figure 2). Regardless of whether **1** was administered to live cells in PBS or in media containing FCS (10%), significant intracellular accumulation of **1** occurs in the macrophages after only 5 min (parts B and D of Figure 2). After 1 h, perinuclear localization of **1** is observed, and this localization does not change with an increasing time of incubation (parts C and E of Figure 2). In contrast, no uptake of the fluorescent cholestenic acid analogue of cholesterol **2** or dansyl sulfonamide **3** (data not shown) is observed over 1 h, whether performed in PBS or media containing FCS (10%).

Previously, we have shown that cultured macrophages cells (J774.1) when treated with atheronal-A and atheronal-B, complexed with LDL, exhibit a time-dependent foamy cellular morphology associated with extensive lipid loading (*4*). The macrophage uptake studies with the fluorescent dansyl hydrazide analogue of atheronal-B **1** are designed to offer real-time insight into the requirements for and gross trafficking of atheronal-B uptake within this cell type. These experiments reveal that the atheronals are efficiently taken up by macrophages, even when not complexed with LDL (parts B and C of Figure 2). This LDL-independent uptake may be of particular relevance in vivo because, under conditions where the atheronals may be generated in an extracellular compartment that is lacking functional LDL, such as is the case within the arterial intima of an atherosclerotic artery, these molecules may still accumulate in the cell, presumably by a receptor-independent pathway and, hence, have their intracellular effects on the macrophage function. In addition, the initial punctate cytosolic accumulation of **1**, followed by its perinuclear accrual within the cell

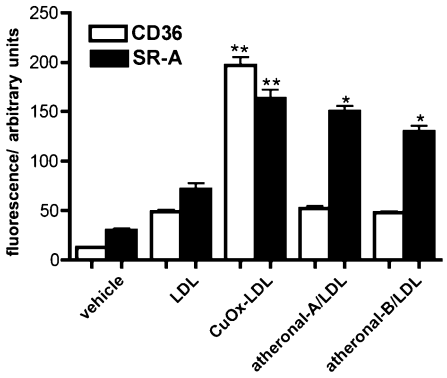

FIGURE 3: Effect of LDL-complexed atheronal-A and atheronal-B on macrophage scavenger receptor expression. Murine macrophage cells (J774A.1) were treated with either vehicle, LDL, CuOx−LDL, atheronal-A (25 μM)/LDL, or atheronal-B (25 μM)/LDL (100 μg/mL protein) for 6 h. Data represent mean fluorescence intensity ± SEM of at least duplicate experiments. (*) $p < 0.05$; (**) $p < 0.01$ versus the control.

hints, suggests that **1** is not being esterified and stored in lipid droplets, which would be localized throughout the cytoplasm (*26*, *27*).

Incubation of cultured murine macrophages (J774A.1) with LDL, complexed with either atheronal-A or atheronal-B, leads to significant upregulation of SR-A. This increase is approximately 3-fold over native LDL ($p < 0.05$) (Figure 3). However, no significant increase in the LDL receptor (CD36) is observed with atheronal complexed with LDL. These data were measured by both indirect flow cytometry and immunoblotting of cellular lysates (see the Supporting Information). Treatment of J774A.1 macrophages with CuOx-LDL (TBARS, 50−75 nmol/mg of protein) results in a significant upregulation of both CD-36 [∼4-fold over native LDL (TBARS, 1−3 nmol/mg of protein, $p < 0.01$] and SR-A [approximately 3-fold over native LDL (TBARS, 1−3 nmol/mg of protein), $p < 0.05$]. In contrast, treatment of cultured macrophages with atheronal-A or atheronal-B alone (data not shown) or the vehicle (PBS and 0.4% DMSO) does not increase the expression of either receptor.

SR-A and CD36 are the main surface receptors responsible for macrophage internalization of modified LDL and oxysterols (*20*, *28*, *29*). It has been shown that both surface receptors are upregulated in the presence of oxidized low-density lipoprotein (ox-LDL) (*30*, *31*), whereas SR-A is upregulated to a higher degree than CD36 in the presence of acetylated LDL (*32*). Thus, the upregulation of SR-A but not CD36 in macrophages in response to treatment with LDL, complexed with either atheronal-A or atheronal-B, suggests a route of internalization for the presumed Schiff base LDL−atheronal adduct highly analogous to that of acetylated LDL.

The combined observations that the fluorescent cholenic acid atheronal-B analogue **1** rapidly accumulates intracellularly within macrophages in the absence of LDL (parts B−E of Figure 2) and that atheronals cause an upregulation of SR-A only when complexed with LDL (Figure 3) suggest that the atheronals are able to enter macrophages by two mechanisms, one of which is surface-receptor-dependent. The second uptake mechanism, while not yet characterized, is presumed to be either passive diffusion or a pinocytotic route.

Incubation of J774.1 cells with either atheronal-A or atheronal-B (6.3−25 μM) in a Boyden chamber leads to macrophage migration by both cholesterol *seco*sterols in a

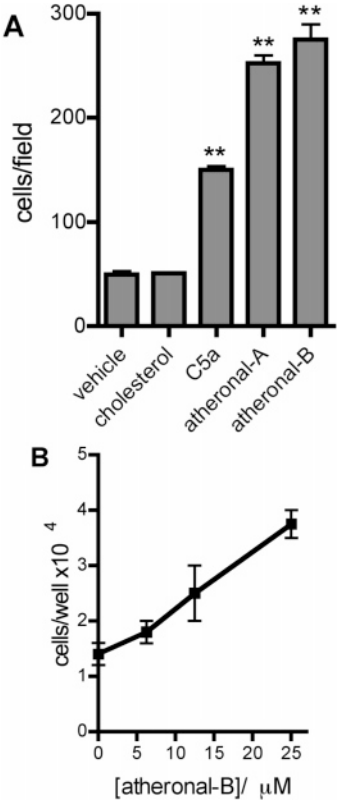

FIGURE 4: Atheronal-induced macrophage chemotaxis. Cultured macrophage (J774.1) cells were treated with either cholesterol (25 μM), C5a (10 nM), atheronal-A (25 μM), or atheronal-B (25 μM) in chemotaxis chambers. (A) Migrated cells were counted using a light microscope and expressed as cells per high-power field. A total of 15 high-power fields were counted for each sample. Cholesterol stimulated migration similar to vehicle control (41 $\pm$ 8 cells/field). Data are reported as the mean $\pm$ SEM of three experiments [(**) $p < 0.001$ versus the vehicle]. (B) Calcein-AM-labeled cells were incubated in the presence of different concentrations of atheronal-B in the lower chambers. Fluorescence of migrated cells was measured by a fluorescence plate reader and expressed as the number of migrated cells/well. Data are reported as the mean $\pm$ SEM of three experiments [(**) $p < 0.001$ versus the vehicle].

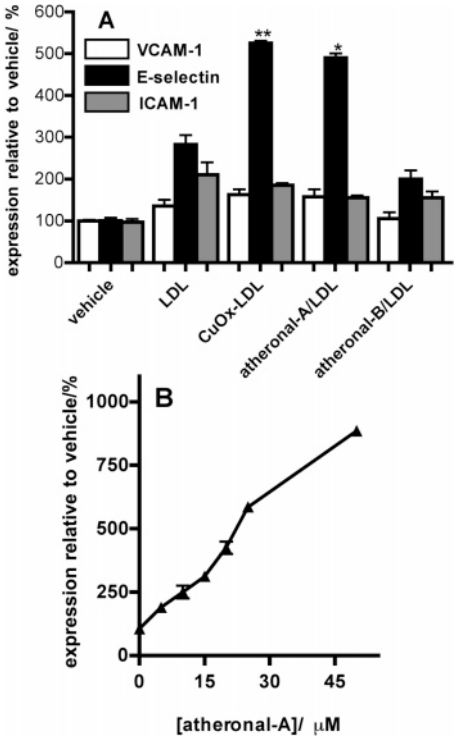

FIGURE 5: Atheronal-induced expression of vascular endothelial cell adhesion molecules. (A) Cultured endothelial cells (HAAE-1) were incubated with LDL, CuOxLDL, atheronal-A (25 μM)/LDL, or atheronal-B (25 μM)/LDL (100 μg/mL protein) for 4 h, and surface expression of VCAM-1, E-selectin, and ICAM-1 was measured by ELISA. Data are reported as the mean $\pm$ SEM from two experiments of the percent expression relative to the vehicle (100%) [(*) $p < 0.05$; (**) $p < 0.005$ versus the vehicle]. (B) Cultured endothelial cells (HAAE-1) were incubated with a range of atheronal-A concentrations (0$-$50 μM) complexed with LDL (100 μg/mL protein), and the surface expression of E-selectin was measured as described in A. Data are reported as the mean $\pm$ SEM of triplicate experiments.

dose-dependent manner ($p < 0.001$; parts A and B of Figure 4). Interestingly, no significant migration of the macrophage cells occurs when atheronal-A or atheronal-B is complexed with native LDL (100 μg/mL; TBARS, 1$-$4 nmol/mg of protein). However, J774.1 cell migration still occurs when atheronal-A and non-LDL are co-incubated with BSA (100 μg/mL; TBARS, 3$-$10 nmol/mg of protein); migration was not suppressed (data not shown). This suppression of atheronal-induced macrophage migration by LDL but not BSA adds further support to our assertion that atheronals complexed to LDL behave in an analogous fashion to ox-LDL, because it is known that macrophages become unable to migrate after accumulation of ox-LDL (*33*, *34*). This effect is used to rationalize why in vivo macrophages become "trapped" in the arterial intima (*35*, *36*).

Macrophages are notoriously slow at replication; therefore, to increase local tissue levels at sites of inflammation, there are a number of naturally occurring chemotactic agents, such as monocyte chemoattractant protein 1 (MCP-1) or leukotriene B4 (LTB-4), that increase leukocyte accumulation at sites of inflammation. Macrophages are by far the major leukocyte present in atherosclerotic arteries, both during atherogenesis progression and at the ultimate thrombotic stage. Thus, the ability of atheronals to recruit macrophages may impact atherogenesis in multiple ways. First, macrophages, already present within the artery wall, may be recruited to sites were the atheronals are being generated extracellularly, leading to areas of high leukocyte density within the plaque, as is known to occur in unstable plaque margins. Alternatively, macrophages containing high levels of atheronals may necrose, leading to the release of atheronals and further recruitment of macrophages to the inflammatory foci. Finally, the atheronals may diffuse from vulnerable sites of the arterial walls, supported by the presence of atheronal-B in the plasma of human atherosclerosis patients. These phenomena would result in a cycle of chemoattractant formation, macrophage chemotaxis, recruitment and activation, and then further chemoattractant formation. This process may well promote the formation and progression of atherosclerotic lesions.

Treatment of vascular endothelial cell (HAAE-1) monolayers with atheronal-A (25 μM) when complexed with LDL (100 μg/mL) causes a >4-fold upregulation of expression of the adhesion molecule E-selectin relative to vehicle control ($p < 0.05$, Figure 5A). In contrast levels of the integrins, VCAM-1 and ICAM-1 remain unchanged. The induction of E-selectin levels by atheronal-A is dose-dependent, with levels increasing from 2-fold at 1.25 μM atheronal-A to ~8-

fold at 50 μM atheronal-A (Figure 5B). This profile of E-selectin upregulation, coupled with no effect upon integrin expression, is the same as observed for CuOx-LDL [(TBARS, 80−100 nmol/mg of protein), $p < 0.005$]. Incubation of endothelial cells with atheronal-B and LDL resulted in upregulation of E-selectin levels (1.8-fold), relative to the vehicle control, similar to those observed with native LDL (~3-fold, multiple experiments tested in triplicate, Figure 5). Administration of atheronal-A or atheronal-B (not complexed with LDL), cholesterol (data not shown), or the vehicle resulted in no effects on either selectin or integrin expression.

Given that atheronal-A when in complex with LDL causes a significant and dose-dependent increase in E-selectin upregulation, with the effect of the atheronals on endothelial cell−monocyte cell, cell−cell adhesion was then assessed using fluorescence spectroscopy. These experiments revealed that neither atheronal-A nor atheronal-B alone or in complex with LDL (1−3 nmol/mg of protein) nor CuOx-LDL (TBARS, 80−100 nmol/mg of protein) significantly increased adhesion of the cultured monocytes cells (U397) to endothelial cell monolayers above that of LDL alone (see the Supporting Information). When the effects of atheronal-A and atheronal-B complexed to LDL on aortic endothelial cell adhesion are taken together, they are highly analogous to that of CuOx-LDL (*24*, *37*). The profile of selectin upregulation but with no effect on integrins and no significant increase in equilibrium binding of monocytes to endothelial cells is consistent with an induction of weak leukocyte−endothelial interactions and is the classic model for induction of leukocyte rolling rather than strict adhesion (*38*), a biological effect that is important in the early stages of inflammatory artery disease.

Previous work by Sevanian and co-workers (*39*) has demonstrated that the oxysterols, 7-KC, 7-hydroxycholesterol, and 22(*R*)-hydroxycholesterol, induce monocyte to macrophage differentiation, while others, such as 25-hydroxycholesterol, do not (*40*). Initial studies studying the effects of cholesterol 5,6-*seco*sterols on cultured human monocytes THP-1 cell differentiation demonstrated that these cells, originally in suspension, began to aggregate in clusters after 24−48 h of atheronal-B treatment. With a longer duration of exposure (~4 days) with atheronal-B (12.5 and 25 μM), a population of cells began to adhere. Within 7 days of culture, the adherent THP-1 cells displayed hypertrophy, developed cytoplasmic vacuoles, and formed extended processes, all characteristic of mature macrophages (parts g and h of Figure 6). These effects of atheronal-B on THP-1 differentiation were exactly mimicked in both the extent and time frame to the positive control of 7-KC (25 μM, parts c and d of Figure 6). In contrast, THP-1 cells treated with either vehicle alone (data not shown), cholesterol (25 μM, parts a and b of Figure 6), or atheronal-A (25 μM, parts e and f of Figure 6) neither became adherent nor developed the aforementioned morphological changes.

The atheronal-B-induced differentiation of the THP-1 cells occurred over a similar time course of human monocyte differentiation in vitro, typically requiring 4−7 days for THP-1 cell-derived macrophages to develop. In addition, the concentration of atheronal-B that causes the determined THP-1 cell differentiation, 25 μM (10.4 μg/mL), is of the same order required for THP-1 cell differentiation by the

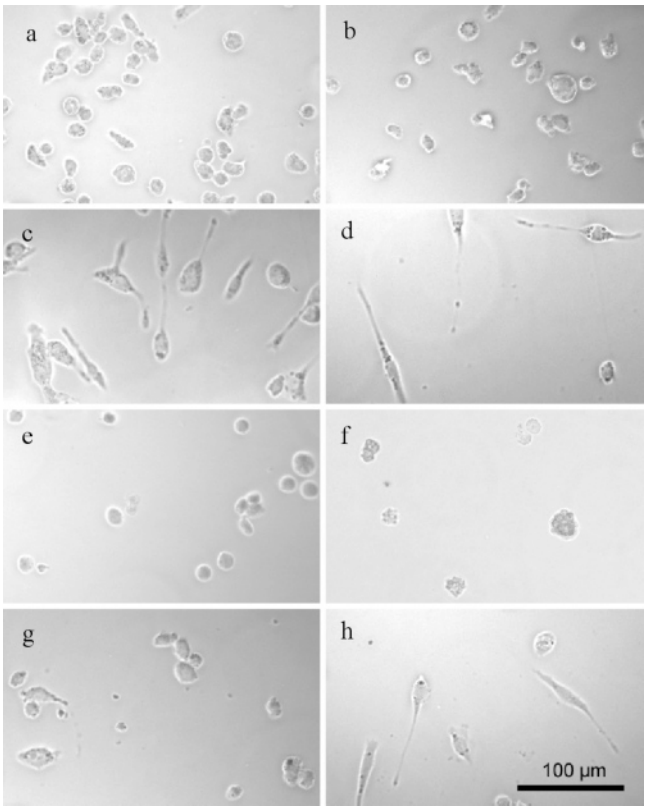

FIGURE 6: Atheronal-induced monocyte differentiation. Cultured human monocyte (THP-1) cells were treated with either 12.5 or 25 μM of the following reagents for a period of 7 days (a and b) cholesterol, (c and d) 7-KC (positive control), (e and f) atheronal-A, and (g and h) atheronal-B. THP-1 cells began to adhere after 4 days of treatment with 7-KC or atheronal-B, and maximal adherence was demonstrated after 7 days. In contrast, cholesterol or atheronal-A treatment induced no cell adherence over the same time frame. Representative phase-contrast microscopy images are shown.

oxysterol 7-KC, suggesting that they are equipotent in this regard (*40*). The mechanism by which atheronal-B induces macrophage differentiation is unclear. However, on the basis of the fact that induction of cell adherence and morphological changes is relatively slow, a mechanism that involves cytokine induction and release seems plausible. It has been previously shown that other oxysterols, including 7-KC, are capable of producing proinflammatory cytokines in other vascular cells, such as monocyte colony-stimulating factor (M-CSF) and granulocyte-macrophage colony-stimulating factor (GM-CSF), if differentiation is slow. The fact that atheronal-B triggers monocyte to macrophage differentiation whereas atheronal-A does not reveals that, while the atheronals share the same chemical composition and a similar structure, they can behave as distinct molecular species.

Evidence that certain oxysterols may contribute to atherosclerosis is accumulating, although a direct link has proven thus far elusive, presumably because of the multifactorial nature of this disease (*41*). Numerous studies have identified elevated levels of oxidized cholesterol derivatives (oxysterols) of both enzymatic (27-hydroxycholesterol) and nonenzymatic (mainly 7-KC and 7-hydroxycholesterol) in plaque tissues, even when expressed relative to parent cholesterol (*41*). Such studies have revealed that the levels of oxysterols are concentrated in foam cells at levels severalfold higher than in plaque as a whole. It has been shown that oxysterols can be present in levels of as much

as 1% of the total cholesterol within atherosclerotic plaque and within foam cells isolated from human atherosclerotic plaque (*42*). For the atheronals, the absolute concentrations within diseased atherosclerotic arteries, with respect to cholesterol, are not known with any degree of certainty at present. However, we have previously shown that plasma levels of atheronal-B can vary from 20 to 500 nM (in cohorts of healthy patients and patients with advanced carotid disease). Given what is known about oxysterol levels in general, we can fairly assume that within the atherosclerotic artery the levels of the atheronals will be significantly higher. The in vitro experiments performed in this study typically focus on atheronal concentration ranges (3−25 μM) that are considered more reflective of levels within the atherosclerotic plaque and foam cells within the plaque rather than equilibrium plasma levels. These levels are considered valid because all of the studies performed are investigating effects that are either triggered within plaque material, such as uptake into macrophages either directly or via macrophage surface receptor upregulation and monocyte to tissue macrophage differentiation, or can be triggered by the leakage of the atheronals from the plaque material to intimately associated cells, such as the vascular endothelial cells.

CONCLUSION

In summary, this paper demonstrates that the products of cholesterol ozonolysis, atheronal-A and atheronal-B, recently discovered in atherosclerotic plaque material, possess biological effects in vitro that may impact atherogenesis and atherosclerosis progression in vivo. The atheronals facilitate macrophage recruitment to vascular tissue, via chemotaxis and endothelial adhesion molecule upregulation. In addition, atheronal-B triggers monocyte to macrophage differentiation and macrophage foam cell formation via scavenger receptor uptake of atheronal-modified LDL. In addition the atheronals can enter macrophages by a receptor-independent process. All of these atheronal-induced in vitro effects are pathological processes ongoing in the context of inflammatory artery disease in vivo.

The proatherogenic properties of the atheronals raise a number of questions in the context of their possible role in atherosclerosis. First, what are the chemical and biological processes within plaques by which these cholesterol oxidation products arise? We have previously shown that activation of inflammatory cells contributes to the acute production of the atheronals in excised atherosclerotic arteries; however, we cannot discount the possibility that atheronals arise chronically, in part, from lung exposure to ozone derived from environmental pollution (*43*, *44*). As such, the atheronals may be a heretofore unrecognized chemical player in the known linkage between environmental pollution and cardiovascular disease. Second, how do these effects, observed in vitro, translate into in vivo models of atherosclerosis? Such studies are ongoing and will be reported in due course.

ACKNOWLEDGMENT

We thank Prof. S. Schmidt (TSRI) for helpful discussion during manuscript preparation and Dr. H. Ditzel (TSRI), Professor L. Gerace (TSRI), and Mr. M. Wood (TSRI) for assistance with fluorescence microscopy.

SUPPORTING INFORMATION AVAILABLE

Immunoblot for CD36 expression, measurement of monocyte−endothelial cell adhesion, extracellular matrix invasion, platelet activation, and Figure S1, monocyte adhesion to endothelial cells. This material is available free of charge via the Internet at http://pubs.acs.org.

REFERENCES

1. Libby, P., Ridker, P. M., and Maseri, A. (2002) Inflammation and atherosclerosis, *Circulation 105*, 1135−1143.
2. Brennan, M. L., and Hazen, S. L. (2003) Emerging role of myeloperoxidase and oxidant stress markers in cardiovascular risk assessment, *Curr. Opin. Lipidol. 14*, 353−359.
3. Brennan, M. L., Penn, M. S., van Lente, F., Nambi, V., Shishehbor, M. H., Aviles, R. J., Goormastic, M., Pepoy, M. L., McErlean, E. S., Topol, E. J., Nissen, S. E., and Hazen, S. L. (2003) Prognostic value of myeloperoxidase in patients with chest pain, *N. Engl. J. Med. 349*, 1595−1604.
4. Wentworth, P., Jr., Nieva, J., Takeuchi, C., Galve, R., Wentworth, A. D., Dilley, R. B., DeLaria, G. A., Saven, A., Babior, B. M., Janda, K. D., Eschenmoser, A., and Lerner, R. A. (2003) Evidence for ozone formation in human atherosclerotic arteries, *Science 302*, 1053−1056.
5. Smith, L. L. (1981) *Cholesterol Autoxidation*, Plenum Press, New York.
6. Wang, K., Bermúdez, E., and Pryor, W. A. (1993) The ozonation of cholesterol: Separation and identification of 2,4-dinitrophenylhydrazine derivatization products of 3β-hydroxy-5-oxo-5,6-secocholestan-6-al, *Steroids 58*, 225−229.
7. Deleted during publication.
8. Zhang, Q. H., Powers, E. T., Nieva, J., Huff, M. E., Dendle, M. A., Bieschke, J., Glabe, C. G., Eschenmoser, A., Wentworth, P., Lerner, R. A., and Kelly, J. W. (2004) Metabolite-initiated protein misfolding may trigger Alzheimer's disease, *Proc. Natl. Acad. Sci. U.S.A. 101*, 4752−4757.
9. Wachtel, E., Bach, D., Epand, R. F., Tishbee, A., and Epand, R. M. (2006) A product of ozonolysis of cholesterol alters the biophysical properties of phosphatidylethanolamine membranes, *Biochemistry 45*, 1345−1351.
10. Rydberg, E. K., Salomonsson, L., Hulten, L. M., Noren, K., Bondjers, G., Wiklund, O., Bjornheden, T., and Ohlsson, B. G. (2003) Hypoxia increases 25-hydroxycholesterol-induced interleukin-8 protein secretion in human macrophages, *Atherosclerosis 170*, 245−252.
11. Liao, H. S., Kodama, T., and Geng, Y. J. (2000) Expression of class A scavenger receptor inhibits apoptosis of macrophages triggered by oxidized low-density lipoprotein and oxysterol, *Arterioscler., Thromb., Vasc. Biol. 20*, 1968−1975.
12. Cader, A. A., Steinberg, F. M., Mazzone, T., and Chait, A. (1997) Mechanisms of enhanced macrophage apoE secretion by oxidized LDL, *J. Lipid Res. 38*, 981−991.
13. Landis, M. S., Patel, H. V., and Capone, J. P. (2002) Oxysterol activators of liver X receptor and 9-*cis*-retinoic acid promote sequential steps in the synthesis and secretion of tumor necrosis factor-α from human monocytes, *J. Biol. Chem. 277*, 4713−4721.
14. Reaven, P. D., Grasse, B. J., and Tribble, J. D. (1994) Effects of linoleate-enriched and oleate-enriched diets in combination with α-tocopherol on the susceptibility of LDL and LDL subfractions to oxidative modification in humans, *Arterioscler., Thromb., Vasc. Biol. 14*, 557−566.
15. Ohkawa, H., Ohishi, N., and Yagi, K. (1979) Assay for lipid peroxides in animal tissues by thiobarbituric acid reaction, *Anal. Biochem. 95*, 351−358.
16. Nichols, W. W., Buynak, E. B., Bradt, C., Hill, R., Aronson, M., Jarrell, B. E., Mueller, S. N., and Levine, E. M. (1987) Cytogenetic evaluation of human endothelial cell cultures, *J. Cell. Physiol. 132*, 453−462.
17. Ralph, P., Moore, M. A., and Nilsson, K. (1976) Lysozyme synthesis by established human and murine histiocytic lymphoma cell lines, *J. Exp. Med. 143*, 1528−1533.
18. Tsuchiya, S., Kobayashi, Y., Goto, Y., Okumura, H., Nakae, S., Konno, T., and Tada, K. (1982) Induction of maturation in cultured human monocytic leukemia cells by a phorbol diester, *Cancer Res. 42*, 1530−1536.

19. Sundstrom, C., and Nilsson, K. (1976) Establishment and characterization of a human histiocytic lymphoma cell line (U-937), *Int. J. Cancer 17*, 565−577.
20. Huh, H. Y., Pearce, S. F., Yesner, L. M., Schindler, J. L., and Silverstein, R. L. (1996) Regulated expression of CD36 during monocyte-to-macrophage differentiation: Potential role of CD36 in foam cell formation, *Blood 87*, 2020−2028.
21. Zwirner, J., Werfel, T., Wilken, H. C., Theile, E., and Gotze, O. (1998) Anaphylatoxin C3a but not C3a(desArg) is a chemotaxin for the mouse macrophage cell line J774, *Eur. J. Immunol. 28*, 1570−1577.
22. Wilkinson, P. C. (1988) Micropore filter methods for leukocyte chemotaxis, *Methods Enzymol. 162*, 38−50.
23. Ng, M. K., Nakhla, S., Baoutina, A., Jessup, W., Handelsman, D. J., and Celermajer, D. S. (2003) Dehydroepiandrosterone, an adrenal androgen, increases human foam cell formation: A potentially pro-atherogenic effect, *J. Am. Coll. Cardiol. 42*, 1967−1974.
24. Khan, B. V., Parthasarathy, S. S., Alexander, R. W., and Medford, R. M. (1995) Modified low-density lipoprotein and its constituents augment cytokine-activated vascular cell adhesion molecule-1 gene expression in human vascular endothelial cells, *J. Clin. Invest. 95*, 1262−1270.
25. Huang, W. C., Chan, S. T., Yang, T. L., Tzeng, C. C., and Chen, C. C. (2004) Inhibition of ICAM-1 gene expression, monocyte adhesion and cancer cell invasion by targeting IKK complex: Molecular and functional study of novel α-methylene-γ-butyrolactone derivatives, *Carcinogenesis 25*, 1925−1934.
26. Ridgway, N. D., Dawson, P. A., Ho, Y. K., Brown, M. S., and Goldstein, J. L. (1992) Translocation of oxysterol binding protein to Golgi apparatus triggered by ligand binding, *J. Cell Biol. 116*, 307−319.
27. Johansson, M., Bocher, V., Lehto, M., Chinetti, G., Kuismanen, E., Ehnholm, C., Staels, B., and Olkkonen, V. M. (2003) The two variants of oxysterol binding protein-related protein-1 display different tissue expression patterns, have different intracellular localization, and are functionally distinct, *Mol. Biol. Cell 14*, 903−915.
28. Nicholson, A. C., Han, J., Febbraio, M., Silversterin, R. L., and Hajjar, D. P. (2001) Role of CD36, the macrophage class B scavenger receptor, in atherosclerosis, *Ann. N.Y. Acad. Sci. 947*, 224−228.
29. Kunjathoor, V. V., Febbraio, M., Podrez, E. A., Moore, K. J., Andersson, L., Koehn, S., Rhee, J. S., Silverstein, R., Hoff, H. F., and Freeman, M. W. (2002) Scavenger receptors class A-I/II and CD36 are the principal receptors responsible for the uptake of modified low-density lipoprotein leading to lipid loading in macrophages, *J. Biol. Chem. 277*, 49982−49988.
30. Yoshida, H., Quehenberger, O., Kondratenko, N., Green, S., and Steinberg, D. (1998) Minimally oxidized low-density lipoprotein increases expression of scavenger receptor A, CD36, and macrosialin in resident mouse peritoneal macrophages, *Arterioscler., Thromb., Vasc. Biol. 18*, 794−802.
31. Han, J., Hajjar, D. P., Febbraio, M., and Nicholson, A. C. (1997) Native and modified low-density lipoproteins increase the functional expression of the macrophage class B scavenger receptor, CD36, *J. Biol. Chem. 272*, 21654−21659.
32. Nakagawa, T., Nozaki, S., Nishida, M., Yakub, J. M., Tomiyama, Y., Nakata, A., Matsumoto, K., Funahashi, T., Kameda-Takemura, K., Kurata, Y., Yamashita, S., and Matsuzawa, Y. (1998) Oxidized LDL increases and interferon-γ decreases expression of CD36 in human monocyte-derived macrophages, *Arterioscler., Thromb., Vasc. Biol. 18*, 1350−1357.
33. Parthasarathy, S., Quinn, M. T., and Steinberg, D. (1988) Is oxidized low-density lipoprotein involved in the recruitment and retention of monocyte/macrophages in the artery wall during the initiation of atherosclerosis? *Basic Life Sci. 49*, 375−380.
34. Quinn, M. T., Parthasarathy, S., Fong, L. G., and Steinberg, D. (1987) Oxidatively modified low-density lipoproteins: A potential role in recruitment and retention of monocyte/macrophages during atherogenesis, *Proc. Natl. Acad. Sci. U.S.A. 84*, 2995−2998.
35. Pataki, M., Lusztig, G., and Robenek, H. (1992) Endocytosis of oxidized LDL and reversibility of migration inhibition in macrophage-derived foam cells in vitro. A mechanism for atherosclerosis regression? *Arterioscler., Thromb., Vasc. Biol. 12*, 936−944.
36. Zerbinatti, C. V., and Gore, R. W. (2003) Uptake of modified low-density lipoproteins alters actin distribution and locomotor forces in macrophages, *Am. J. Physiol. Cell Physiol. 284*, C555−C561.
37. Vielma, S. A., Mironova, M., Ku, J. R., and Lopes-Virella, M. F. (2004) Oxidized LDL further enhances expression of adhesion molecules in *Chlamydophila pneumoniae*-infected endothelial cells, *J. Lipid Res. 45*, 873−880.
38. Charo, I. F., Bekeart, L. S., and Phillips, D. R. (1987) Platelet glycoprotein IIb-IIIa-like proteins mediate endothelial cell attachment to adhesive proteins and the extracellular matrix, *J. Biol. Chem. 262*, 9935−9938.
39. Hayden, J. M., Brachova, L., Higgins, K., Obermiller, L., Sevanian, A., Khandrika, S., and Reaven, P. D. (2002) Induction of monocyte differentiation and foam cell formation in vitro by 7-ketocholesterol, *J. Lipid Res. 43*, 26−35.
40. Hayden, J. M., Brachova, L., Higgins, K., Obermiller, L., Sevanian, A., Khandrika, S., and Reaven, P. D. (2002) Induction of monocyte differentiation and foam cell formation in vitro by 7-ketocholesterol, *J. Lipid Res. 43*, 26−35.
41. Brown, A. J., and Jessup, W. (1999) Oxysterols and atherosclerosis, *Atherosclerosis 142*, 1−28.
42. Brown, A. J., Leong, S. L., Dean, R. T., and Jessup, W. (1997) 7-Hydroperoxycholesterol and its products in oxidized low-density lipoprotein and human atherosclerotic plaque, *J. Lipid Res. 38*, 1730−1745.
43. Pulfer, M. K., Taube, C., Gelfand, E., and Murphy, R. C. (2005) Ozone exposure in vivo and formation of biologically active oxysterols in the lung, *J. Pharmacol. Exp. Ther. 312*, 256−264.
44. Pulfer, M. K., and Murphy, R. C. (2004) Formation of biologically active oxysterols during ozonolysis of cholesterol present in lung surfactant, *J. Biol. Chem. 279*, 26331−26338.

BI0604330